Conference Paper, Published Version

David, Gabriel; Schlurmann, Torsten; Roeber, Volker

Coastal Infrastructure on Reef Islands – the Port of Fuvahmulah, the Maldives as Example of Maladaptation to Sea-Level Rise?

Coastal Structures 2019 - Nils Goseberg, Torsten Schlurmann (eds) - © 2019 Bundesanstalt für Wasserbau
ISBN 978-3-939230-64-9 (Online) - DOI: 10.18451/978-3-939230-64-9_087

Coastal Infrastructure on Reef Islands – the Port of Fuvahmulah, the Maldives as Example of Maladaptation to Sea-Level Rise?

C. G. David & T. Schlurmann
Leibniz Universität Hannover, Ludwig-Franzius-Institut for Hydraulic, Estuarine and Coastal Engineering, Hannover, Germany

V. Roeber
Univ Pau & Pays Adour / E2S UPPA, Chaire HPC-Waves, Anglet, France

Abstract: Infrastructure and the development of logistics are a pre-requisite for economic growth in remote islands. Air and seaports are important hubs in the exchange of cargo and transfer of passengers in any logistic transport network. Once designed and constructed, seaports interfere with the local hydro- and morphodynamic system and potentially affect adjacent coastal areas. Small reef islands are particularly sensitive towards sea-level rise and impacts due to coastal structures as implementation may increase their exposure and increase the vulnerability of the local population, if infrastructure development compromise or even imperil the natural equilibrium. This study documents and validates the erosion on the east coast of the Maldivian coral reef island of Fuvahmulah. Two numerical models help to identify the key drivers and interdependent processes of sediment transport on the coral reef and assess the port's influence in aggravating formerly balanced sediment budgets. Our results highlight the significant susceptibility of reef islands in regard of inherent coastal processes as it calls for thoughtful investigations in the design stage prior to implementation of coastal infrastructures in order to avoid any misdesigning of seaports or even to maladaptation practices in remote islands.

Keywords: Erosion, sediment transport, reef island, numerical modelling, hindcast data-set

1 Introduction

Small islands and atolls are particularly exposed to sea-level rise and its associated impacts, as they are situated shortly above mean sea-level, while being completely surrounded by the sea. Communities of small islands are particularly vulnerable as they lack options for retreat (Nurse et al., 2014). AR5 of IPCC (2013) states that with high to very high confidence, coastal risks for low-lying areas will increase. Storlazzi et al., (2015, 2018) show, that due to global warming, this could translate to uninhabitable atolls in a few decades. Albert et al. (2016) report severe shoreline recession on the Solomon Islands. In contrast, McLean and Kench (2015 present varying trends in net land area change for 12 islands in the central and western Pacific over 116 years, including positive sediment budgets despite sea-level rise (SLR). Kench and Brander (2006) as well as Kench et al. (2009) describe inherent coping capacities of reef islands against sea-level rise and wave impact due to high morphodynamic activity. These studies find high changes in the inter-seasonal sediment budget, but annual net-changes are much smaller or at equilibrium.

Coastal structures and anthropogenic interventions disrupt the natural equilibrium of the beach (Kamphuis, 2000; Ranasinghe and Turner, 2006; Luijendijk et al., 2018). In the case of small islands, such a disturbance can potentially create additional stress for the island and increase vulnerability of the coastal system towards SLR (Lewis, 1990; Pelling and Uitto, 2001; Magnan et al., 2016). Increasing (future) vulnerability towards SLR by any form of changes is the general definition of maladaptation to climate change (Magnan et al., 2016). This study presents the case of the Maldivian island Fuvahmulah (Latitude: -0.30°, Longitude: 73.42°), suffering from erosion after the construction of the local seaport. The port was the first of a number of projects to improve Fuvahmulah's

infrastructure. The port construction has led to erosion on the eastern side of the island. This study will investigate the intensity of the erosion based on three field campaigns. In order to reveal factors leading to erosion, two numerical models will examine the interaction of waves, bathymetry and sediment. Ultimately, this study presents the lessons learned from the example of Fuvahmulah and provides important insights in planning and designing coastal structures in reef island environments to avoid maladaptation.

2 Methods

The following subsections explain our workflow to quantify erosion, the data used as boundary conditions and the settings of the numerical models. Summarized, the subsections contain:

- An introduction to the study site and steps taken from aerial photos to create a digital elevation model (DEM).
- The considered ocean wave hindcasts, derived wave input for the numerical models and information on ocean circulation and tidal currents.
- Settings and purpose of the coarse D3D model and the high resolution, depth averaged (2DH) Boussinesq-type model.

2.1 Study Site

Fuvahmulah is an island in the Maldives, located approximately 30km south of the equator (see Fig. 1). The island's recent development led to the construction of a local port in the south-eastern part of the island (completed in 2002) and a domestic airport in the south-west (completed in 2011). The trademark of Fuvahmulah among Maldivian islands is its sandy beach Thoondu. Thoondu is situated in the north of the island. But as wave direction changes with the seasons, Thoondu wanders from the north to the north-east of the island and vice versa. The north is morphodynamically very active and the beach face can alter within a few weeks. This phenomenon as well as the constant change of Thoondu is well known to locals. Unlike Thoondu, the lower east coast of Fuvahmulah was regarded stable. But since the port was built, the whole east-side up until Thoondu faces erosion (Naeem, 2006).

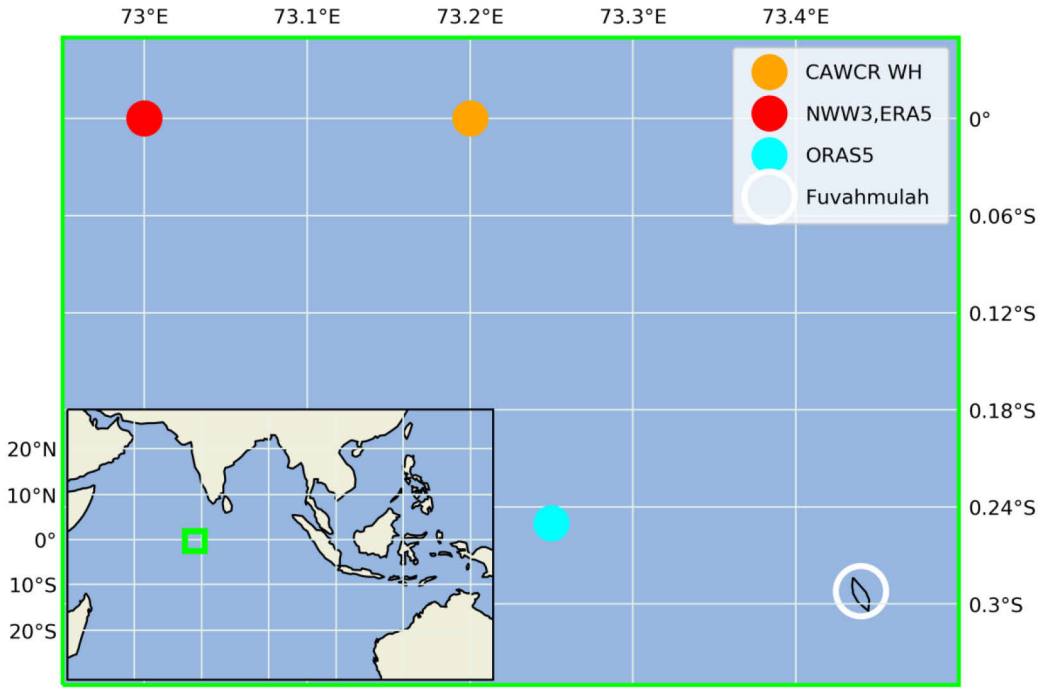

Fig. 1. Model area in global (black box) and regional context (green box). The encircled, white area is the location of Fuvahmulah. Green and orange circles mark the output nodes of the ocean wave hindcast for each of the three available models. The blue circle is the output node of the ocean circulation model, which is used to derive meridional and zonal velocities.

We were able to record aerial photos with a DJI Phantom 4 drone in our field campaigns in March 2017, September 2017 and March 2019. With the help of Agisoft Photoscan Pro, the aerial photos result in a digital elevation model. The general workflow in Photoscan is to align the photos, georeferencing the model by Ground Control Points (GCP) and creating a dense point cloud as well as a mesh of the area. Photoscan derives the DEM from the dense point cloud, while the mesh serves as base for the orthophoto. A unique set of GCPs will be used for the March 2019 DEM in future studies. However, the GNSS data is still being processed for this study. The comparison between the 2017 and 2019 model will use the drone's GNSS antennas for initial positioning. Afterwards virtual GCPs of specific landmarks available in both models georeference the models with each other. This could lead to position errors of the 2019 model when compared to the location in a georeferenced coordinate system. However a direct comparison between both models has no signal and measurement errors and allow for a better intercomparison between the two models.

2.2 Hydrodynamic boundary conditions

In a next step, this study derives hydrodynamic boundary conditions from ocean wave hindcast models. As Fig. 1 shows, the output node of the CAWCR Wave Hindcast of the Australian Commonwealth Scientific and Industrial Research Organisation (CSIRO) is closest to the island. Durrant et al. (2013) provide ocean wave data from a WAVEWATCH III model on global grid with a resolution of 0.4°x0.4° for a period of 32 years (1979-2010). The waves were forced with Climate Forecast System Reanalysis v.2 (CFSv2) surface winds at 0.2° spatial and hourly temporal resolution. The data was cross-checked with similar data sets provided by the American National Oceanic and Atmospheric Administration (NOAA, also uses the WaveWatchIII engine with bias corrected CFSR wind forcing) and the European Centre for Medium-Range Weather Forecasts (ECWMF, WAM-model with forcing from ECMWF's Integrated Forecast System; C3S, 2017). The analysis of the CAWCR data-set yielded in a wave rose, shown in Fig 2.

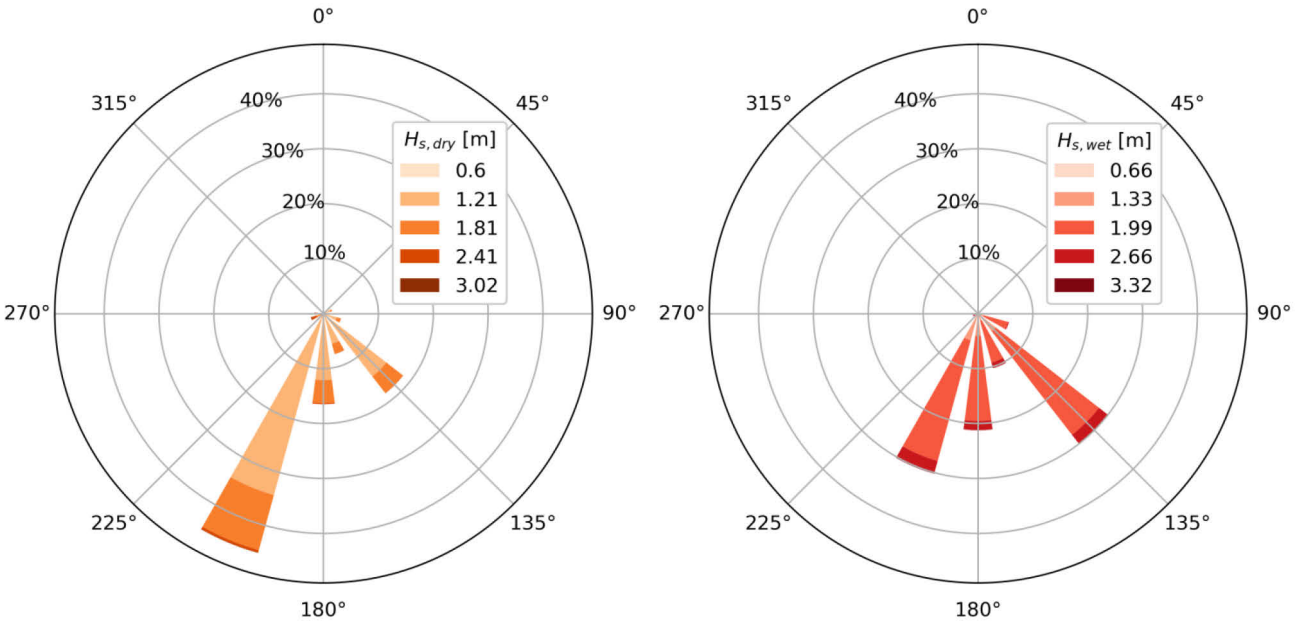

Fig. 2. Wave rose for Fuvahmulah, separated for dry season (left, November to Feburary) and wet season (right, April to September). The wave roses contain the significant wave height H_s from the CAWCR dataset, separated in 5 bins. The legend shows the maximum H_s of each bin.

The wave rose shows the wave climate in the area around Fuvahmulah for the dry and wet season. This study defines the period between November to Feburary as dry season and the period between April and September as wet season. April and October are considered transition months. The waves are smaller in dry season and are dominantly approaching the island from SSE (202.5 °). There are southern and south western portions, but in terms of occurrence they play a lesser role. In general significant wave heights H_s are smaller than 1.81m. The reanalysis data set contains higher significant wave heights in dry season, but they appear rarely. In rainy season, SW and SSE (135° and 202.5°)

are the two dominant wave directions. Waves from south occur more often than in dry season, but are still not considered dominant. In rainy season significant wave heights increase and are mostly between H_s=1.34-1.99m. This study looks at wave propagating from SW and SSE into the area, because in both seasons they represent the two dominant shares of the wave rose for Fuvahmulah. The numerical models use the 99th percentile from the reanalysis data set (H_s=2.3m) as boundary condition. All conditions are therefore modeled for storm conditions.

As this study focuses on the wave driven longshore currents, ocean circulation around Fuvahmulah and the tidal current velocity will be disregarded. In this region, the median ocean circulation velocity is $v_{m,oceancirc.}$ = 0.40ms^{-1} while the median tidal current velocity is $v_{m,tide}$=0.10 ms^{-1}. The velocity of the ocean circulation was derived from monthly means of the ORAS5 ECMWF reanalysis data-set. The reanalysis data set calculates ocean (thermo-)dynamics and provides zonal and meridonal velocities between 1979-2017 at the position marked in Fig. 1. The tidal velocities were taken from a coarse Delft3D model and show two peaks on the north-west ($v_{max,tide}$=0.30ms^{-1}) and south east-side (v_{tide}=0.28 ms^{-1}) of the island. According to Burcharth et al. (2007) these components is standard practice when regarding longshore sediment transport. They state, that longshore sediment transport mainly depends on incident waves, while tidal and ocean currents are of minor importance.

2.3 Numerical Tools

First, we use Delft3D (D3D) to understand the general sediment transport processes around the island. D3D has been used successfully for calculating sediment transport and demonstrated good performance in both experimental and hindcast studies (Roelvink, 2006; Lowe et al., 2009; van der Wegen and Roelvink, 2012. Therefore, the model is capable to compute the morphodynamic processes on the Fuvahmulah reef. In order to remain numerically stable and efficient in terms of computational resources the model is based on the following simplifications: The model uses a coarse grid, with a refined resolution of Δx=67m, Δy=15m around Fuvahmulah. Delft3D uses both the WAVE and the FLOW module (Lesser et al., 2004; Holthuijsen, 2010) to study the morphodynamic processes around the island. The bathymetry is idealized with an off-shore section subject to a constant water depth of h=100m. The reef has a constant depth of h=4m and Fuvahmulah lies at 2m above MSL. The off-shore reef south of the island has a similar shape in the model compared to the real reef. However to provide enough cells to transport sediment, the fringing reef in the model is wide. The implementation is still sufficiently detailed to see the interaction between bathymetry, waves and sediment on the reef. To calculate the tidal current velocity in the region, the first simulation used a time-series of the neighboring Gan tide gauge (~53 km away from Fuvahmulah).

The following simulations in D3D use a PM-spectrum with H_s=2.3m, T_p=17s and a peak direction of θ_p =202.5° and θ_p =135° respectively. We acknowledge the complexity of sediment transport on coral reefs (as shown for example in: Storlazzi et al, 2011; Pomeroy et al., 2015). However for a first estimation, D3D runs only with the (suspended and bed-load) sediment transport formulations as described by van Rijn (1993) and Lesser et al. (2004). All simulations use the same sediment properties: The sediment layer thickness is d_{sed}=1m, sediment density is $\rho_{sed.}$1600 kg/m3 and sediment grain size (diameter) is D=200µm. The morphological scale factor is f_{MOR}=2.

For the detailed study of the port, we use a depth-averaged Boussinesq-type model as presented in Roeber and Cheung (2012). The reef bathymetry in this model was recorded with a single-beam echo-sounder during the first field campaign in 2017. The echo-sounder had a maximum range of up to approximately 45m water depth, while the minimum depth was 4m due to the draft of the boat. The 2017 Photoscan model provides the island topography and nearshore bathymetry at about MLT to MSL. The Generic Mapping Tool (Wessel and Luis, 2017) grids the elevation data on a 7.5m by 7.5m grid. Offshore waters are 60m deep. Similar as before, we use a wave spectrum with H_s=2.3m, T_p=17s and a peak direction of θ_p =202.5° and θ_p =135° respectively.

3 Results

The digital elevation model quantifies the erosion along the east coast. Fig 3 shows the same cross-section in 2017 and 2019 about 260m north of the seaport. The upper part at L=1.8-2.2m shows erosion of about 30 - 40cm. The 2017 cross section contains a coral rock at L=5m. The rock is visible in the dense point cloud of the 2017 model (Fig. 3) and washed away in the 2019 model. Adjacent to

the cross-section was a palm tree, that later fell onto the reef. There are further instances of uprooted trees along the south-eastern part of the island. Large parts of Fuvahmulah's coast have a coastal forest, reinforcing the beach profile. Other sections consist of huge coral rocks. Waves and currents carve out the sediment under the roots or dislocate coral rocks. These observations show, that on the east side of Fuvahmulah, erosion starts at the bottom of the profile. Erosion remains undetected in

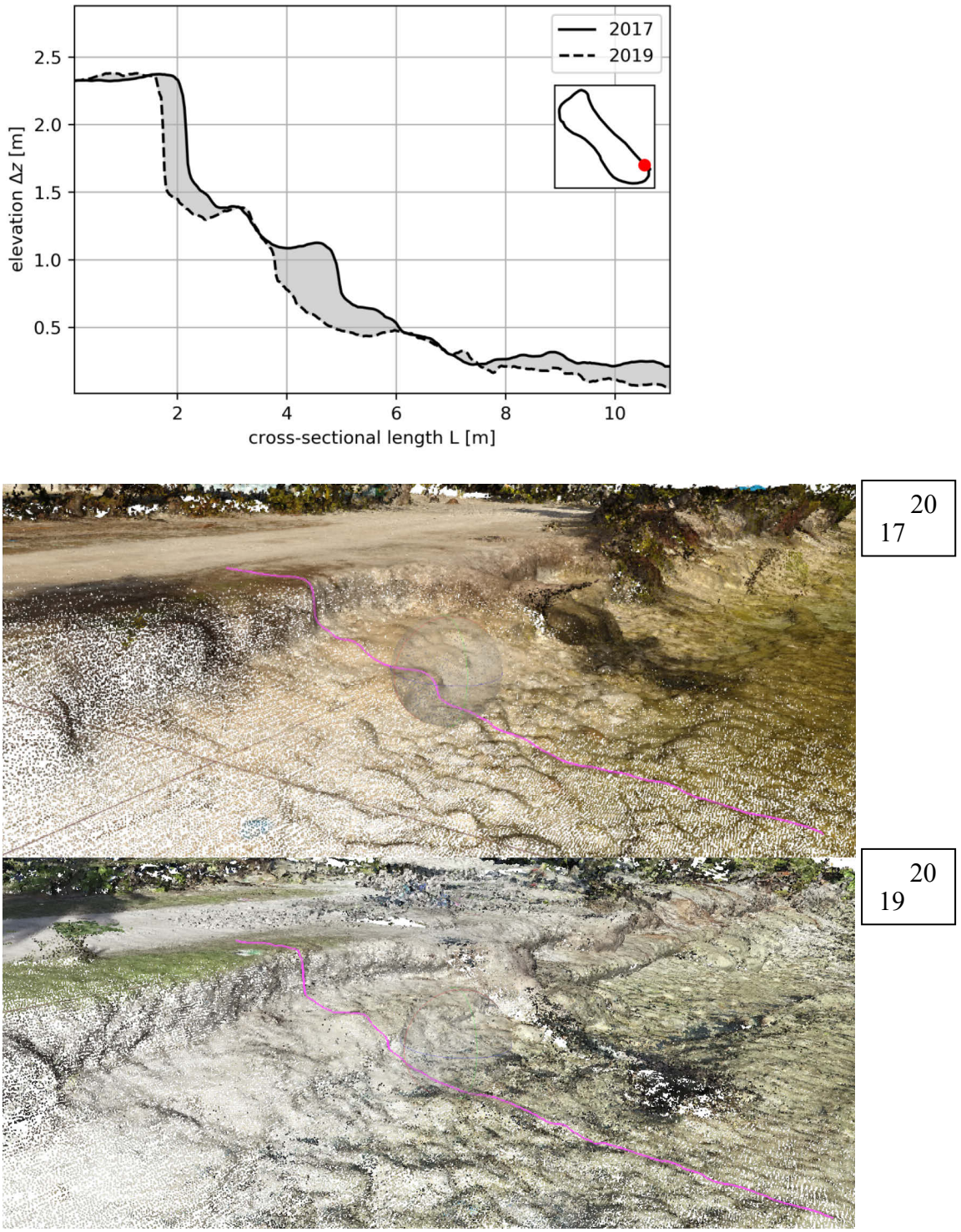

Fig. 3. Beach profile (top) and dense point cloud (middle 2017. Bottom 2019) processed by Agisoft Photoscan from the aerial photos. The pink line in the dense point cloud corresponds to the cross section in the top figure. In the top figure, the red dot on the mini-map of Fuvahmulah indicates the location of the cross section. The cross-sections are in close proximity of the port.

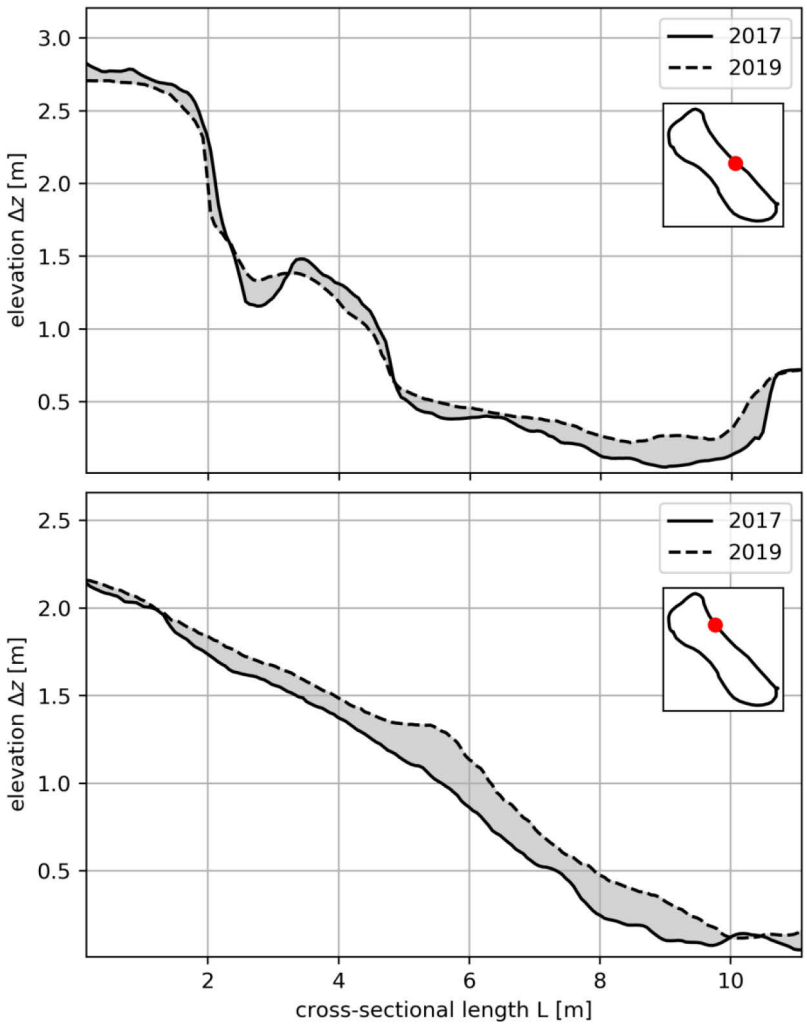

Fig. 4. Beach profile processed by Agisoft Photoscan from the aerial photos. The red dot on the mini-map of Fuvahmulah indicates the location of the cross section. The top figure shows a cross section in the central area of the east coast while the bottom figure shows a cross-section in the north-east part in close proximity of Thoondu.

DEMs until the upper part slips or collapses. DEMs need much more information and processing time to visualize this type of erosion. The erosion is advanced enough to be noticed in the DEM. Collapsed or dislocated blocks are clearly visible in the photogrammetric models: Fig 4 (top) shows a dislocated reef block at L=3.45m (2017) and L=3.29m (2019). The block is Δz=0.12m higher in 2017 and the off-shore facing front of is steeper than in the 2019 profile. Erosion can still be measured at this location, but the beach erodes much slower than at the south-eastern profile in Fig 3. Fig 4 (bottom) shows a beach profile in the north east of the island, where no significant erosion is visible. The transections in Fig.3 and Fig. 4 have shown that the DEM provide valuable information to quantify the cross-sectional erosion. It has also shown, that erosion is severe in the south-east of the island and declines along the east coast.

D3D helps to put the observations from the DEM in context with the hydrodynamic forcing from the reanalysis data set. D3D calculates the sediment shift for different wave directions over a period of one month. The erodable sediment layer was 1m throughout the domain. Figure 5 shows the model output for storm waves from SW and SSE:

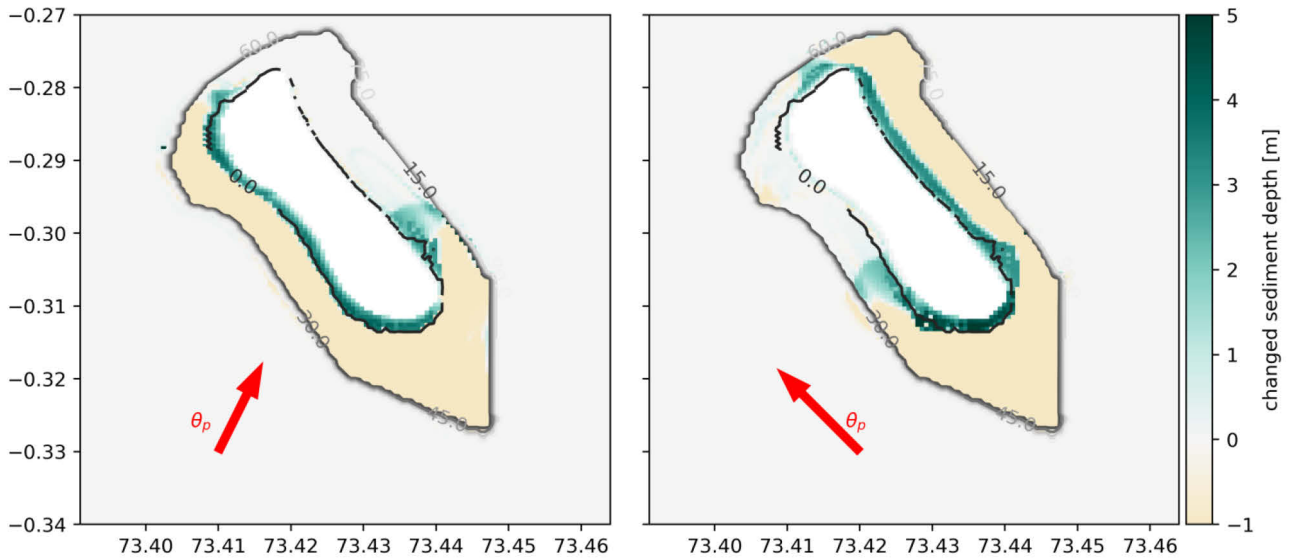

Fig. 5. Cumulative sedimentation and erosion computed by D3D for H_s=2.3, T_p=17s. and a modelling time of one month. The left figure shows cumulative sedimentation / erosion for waves coming from θ_p=202.5°, the right figure for waves with a peak direction of θ_p=135°.

As waves approach from 202°, sediment moves on the reef towards the island and settles on the west side. A smaller sediment depot also forms on the south east of the island. On the other hand, waves from 135° will take sediment from the offshore reef and distribute it on the south side and along the east coast of the island. A small portion of the sediment will also accumulate on the south west side. In case, sediment on the lee side of the island will not be affected.

D3D does not contain port structures in its bathymetry. It will also enlarge the area of sedimentation, as the fringing reef is wider than in reality. As a result, the coarse D3D model only shows the typical morphodynamic behavior for an environment like the Fuvahmulah reef. It shows that the reef is the sediment source for Fuvahmulah and indicates where to expect sediment deposits under the given hydrodynamic forcing. From the D3D model, it becomes obvious, that without the port, there is a constant sediment supply from the port along the east coast. D3D also shows, that the south-east part of the island is of particular interest for sediment transport along the entire east coast. However due to the coarse resolution and the idealized bathymetry, the model does not show the influence of the port in detail.

To overcome this, a 2DH model highlights the difference in wave driven current patterns around the port area. This approach has to be interpreted with caution, because erosion or sedimentation depend on more factors than current velocities. However current velocities and velocity gradients can hint at potential transport rates as well as erosion and sedimentation hotspots. The 2DH model reveals two factors, contributing to the erosion along the east coast of the island:

The first factor is the available sediment: Fig 6 shows the computed mean velocity uv_{mean} with and without the port structures (breakwater and headland). In both cases, waves from θ_p=202.5° create a current in front of the port and a decelerated area at today's port entrance. D3D has shown, that for waves from θ_p=202.5°, sediment will accumulate on the south-east of the island. The current in front of the port transports sediment over the reef, while velocity gradient in the port area allows for the sediment to accumulate in this area. However with the breakwater present, sediment cannot enter this area. In addition, the breakwater reaches up to the reef edge. It deflects the current, and thus the sediment off the reef into deeper waters.

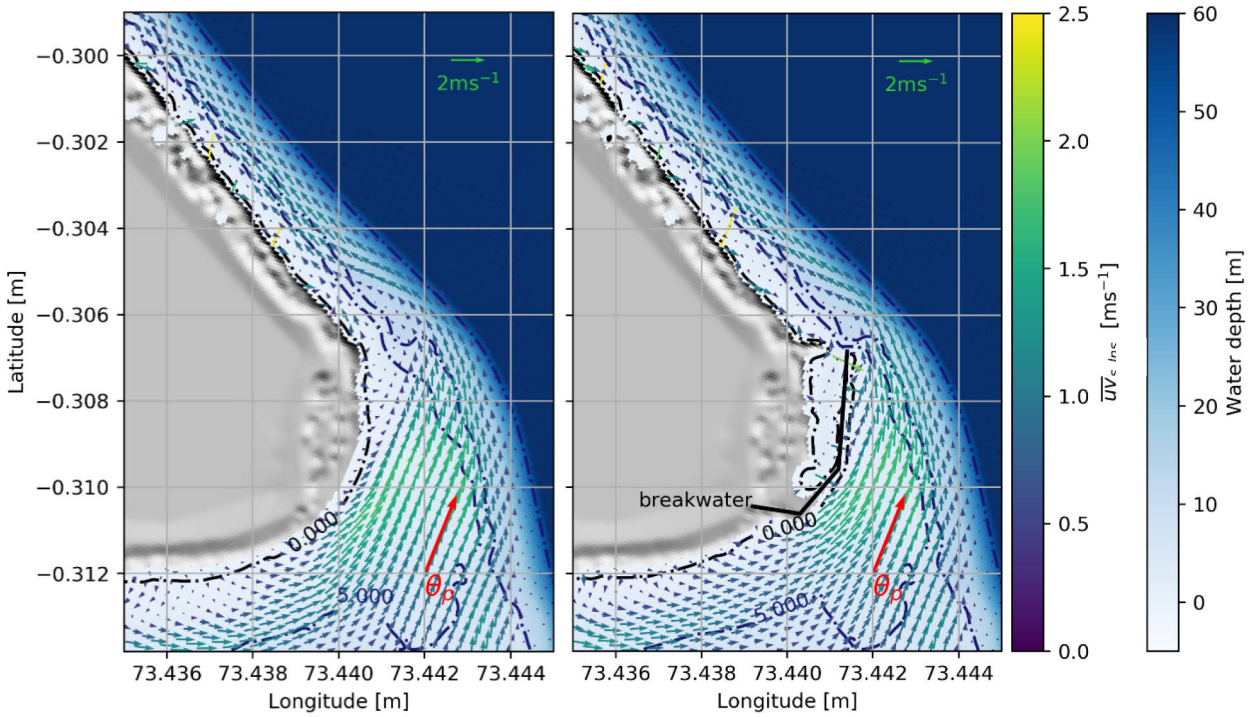

Fig. 6. Mean velocities uv_{mean} from the 2DH model are displayed with arrows according to the left colorbar. Blue colors show the underwater bathymetry, while the gray area is a shaded model of the island topography with elevation > 0m. Bottom contours for 0, 5, 10 and 60m water depth are blue dash-dotted lines. The red arrow indicates the peak frequency of θ_p=202.5°.

The second factor is the transport capacity of the east-coast current: Without breakwater, waves with θ_p=135° induce a northward current into the area of today's port entrance (see Fig. 7). This is also the area, where sediment was able to settle from the 202.5° component. Instead, the breakwater obstructs the current to evolve in this area and deflects the velocity momentum off-shore. Anyway, a longshore current is present on the east coast independently of the port: Breaking waves from 135° will approach the reef at an angle, inducing radiation stresses and subsequently a longshore current. With missing sediment from the reef, the currents will very likely take sediment from the coast, leading to erosion.

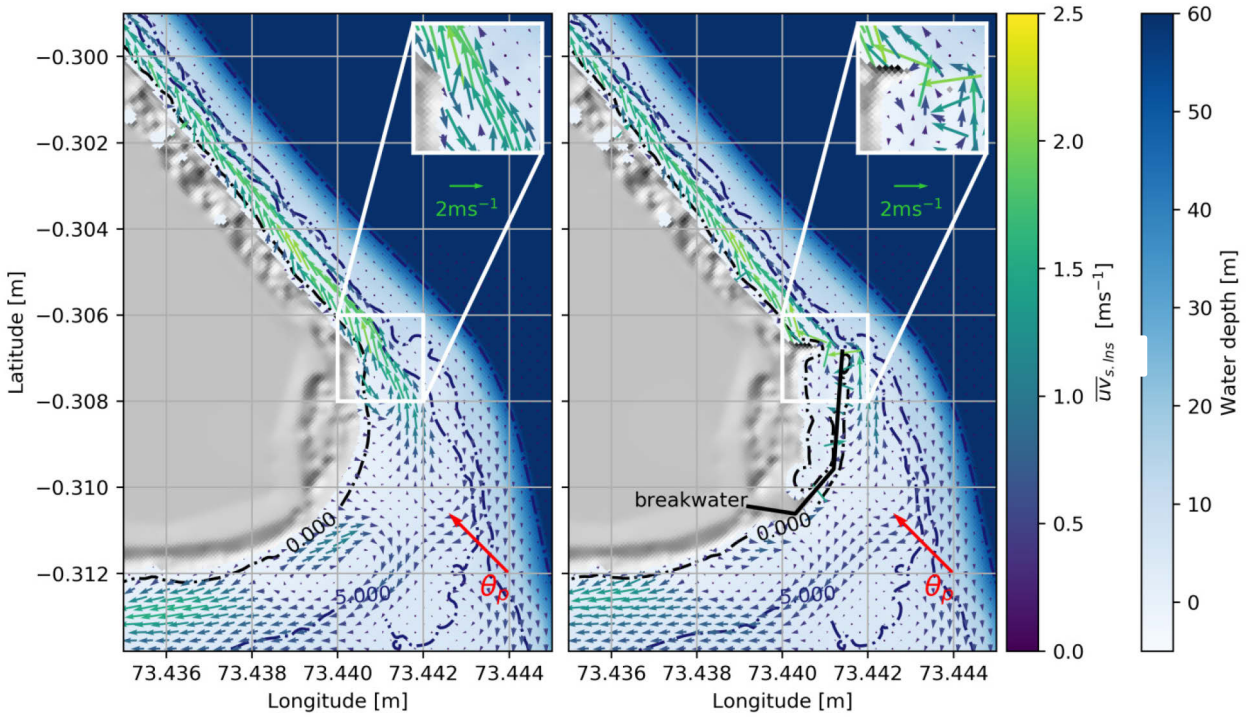

Fig. 7. Mean velocities uv_{mean} from the 2DH model are displayed with arrows according to the left colorbar. Blue colors show the underwater bathymetry, while the gray area is a shaded model of the island topography with elevation > 0m. Bottom contours for 0, 5, 10 and 60m water depth are blue dash-dotted lines. The red arrow indicates the peak frequency of θ_p=135°. The zoomed tile shows velocities at the port entrance with and without the structure. The model shows high velocities at places, where waves overtop the breakwater.

Both numerical models show, that the most severe impact of the port is its barrier function for the sediment. This is exaggerated by the fact, that longshore currents take away the remaining sediment north of the port. A solution for the situation would be to allow sediment to pass the barrier. However, the port will still influence the velocity for a major part of the east coast.

Fig. 8 shows the difference of uv_{mean} before the construction of the harbor, compared to the present situation with harbor. Positive values indicate faster velocities without the port. Without interference of coastal infrastructure, the velocity difference is +0.73ms^{-1} behind the port entrance. Therefore, sediment which has passed the breakwater in the current situation (for example through a sand bypass or suction dredging) and was in suspension, may not propagate as far as before (this assumption is based on the fact, that decelerated depth-averaged velocity reduces the total sediment transport as stated in the Soulsby-van Rijn formula; Soulsby, 1997). In this case, erosion would be mitigated but the bypass would probably not restore the original conditions.

These findings suggest that planning coastal structures in a reef environment underlies special requirements. Unlike for longer stretches of continental shelfs, reef islands have a closed morphodynamic system. Sediment sources and sinks can easier be identified in these systems. However the example of Fuvahmulah has shown, that modifications to this system also have more significant implications for greater portions of the coast. In the context of SLR, small islands are especially vulnerable towards coastal hazards. Erosion poses further pressure on coastal communities ‘downstream’, which have either no or very limited options for retreat. As consequence, erosion will increase the vulnerability of the affected areas towards coastal hazards, which is the generally recognized definition of maladaptation (Magnan et al., 2016). Therefore, this study concludes, that in the face of SLR, planning coastal infrastructure on reef islands requires a holistic design approach for the reef, to avoid adverse impact on nearby areas.

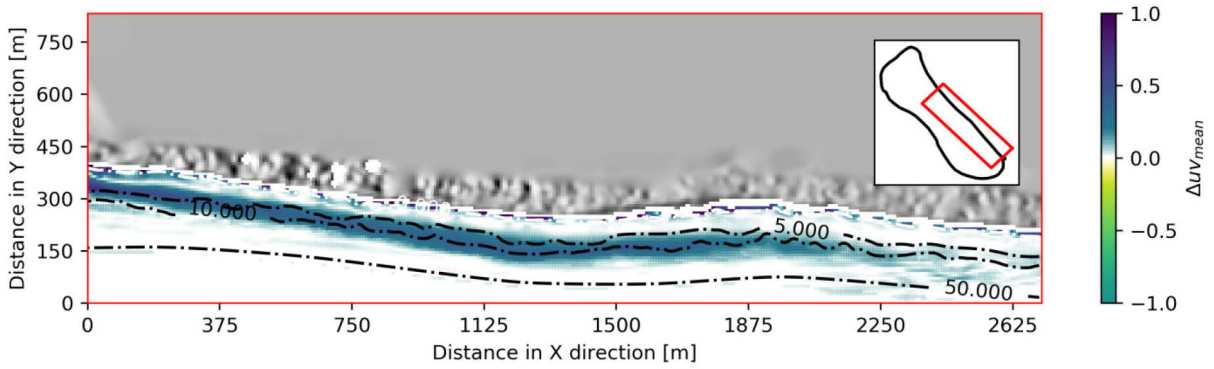

Fig. 8. Velocity difference Δuv_{mean} from the 2DH model for the central and south-east coast of Fuvahmulah. Positive values indicate decreased current velocities due to the presence of the port. The red box in the mini-map of Fuvahmulah shows the study area.

4 Conclusion

The purpose of the study is to measure the severity of erosion on the east side of Fuvahmulah. This study also identifies the main drivers for sediment transport on the offshore and fringing reef of the island. Understanding the main processes allows to estimate the impact of the port on the hydro- and morphodynamic system.

The investigation reveals, that the south-east side of Fuvahmulah experiences strong erosion. The numerical models identify the area of today's port as potentially critical location for sediment transport on the east side of the island. The 2DH model also shows, that the port acts as barrier and deflects suspended sediment off the reef, which otherwise would have been transported along the east side of the island.

Some limitations apply to the conclusion of these results: for example the wave input is based on storm wave heights of two peak directions. Also, the distribution of sediment will not depend solely on storm events. Furthermore, there was no evaluation of the in-situ sediment parameters. Consecutive studies must therefore answer how the system responds to more differentiated assumptions.

However in the end, this study provides the first comprehensive evaluation of the morphodynamic system of the Fuvahmulah reef. It shows, that the morphodynamic system is closed and only forced by the hydrodynamic boundary conditions. It reveals the significance of a holistic design approach for coastal infrastructure on reef islands as well as the risk of maladaptation of adjacent areas by mis-designing the coastal structures of the port.

5 Acknowledgements

The authors thank Pablo Ballesteros, Zahid Abdul Hameed-Elhagedar, Rene Klein, Nina Kohl, Manó Schütt and Ali for their support on the Maldives. We also acknowledge Astrid Kartes and Jannek Gundlach, supporting us with D3D. Finally we are grateful for the feedback and the discussions with the sediment group of LuFI, led by Jan Visscher.

C. Gabriel David and Torsten Schlurmann work within the DICES project as part of the Priority Program (SPP-1889) 'Regional Sea Level Change and Society (SeaLevel)', funded by the German Research Foundation (Deutsche Forschungsgemeinschaft, DFG). Volker Roeber acknowledges financial support from the Isite program Energy Environment Solutions (E2S), the Communauté d'Agglomération Pays Basque (CAPB) and the Communauté Région Nouvelle Aquitaine (CRNA) for the chair position HPC-Waves.

References

Albert, S., Leon, J. X., Grinham, A. R., Church, J. A., Gibbes, B. R., and Woodroffe, C. D., 2016. Interactions between sea-level rise and wave exposure on reef island dynamics in 130 the solomon islands. Environmental Research Letters, 11(5):054011

Burcharth H. F., Hawkins S. J., Zanuttigh B., Lamberti A., 2007. Design tools related to engineering. In Hans F. Burcharth, Burcharth H. F., Hawkins S.J., Zanuttigh B., Lamberti A, editors, Environmental Design Guidelines for Low Crested Coastal Structures, pages 203 – 333. Elsevier Science Ltd, Oxford, 2007

Copernicus Climate Change Service (C3S), 2017. ERA5: Fifth generation of ECMWF atmospheric reanalyses of the global climate . Copernicus Climate Change Service Climate Data Store (CDS), date of access. https://cds.climate.copernicus.eu/cdsapp#!/home

Durrant, Thomas; Hemer, Mark; Trenham, Claire; Greenslade, Diana, (2013. CAWCR wave hindcast extension Jan 2011 - May 2013. v4. CSIRO. Data Collection. https://doi.org/10.4225/08/52817E2858340

Holthuijsen, L., 2010. Waves in Oceanic and Coastal Waters. Cambridge: Cambridge University Press. doi:10.1017/CBO9780511618536

IPCC, 2013. Summary for policymakers. In Field, C., Barros, V., Dokken, D., Mach, K., Mastrandrea, M., Bilir, T., Chatterjee, M., Ebi, K., Estrada, Y., Genova, R., Girma, B., Kissel, E., Levy, A., MacCracken, S., Mastrandrea, P., and White, L., editors, Climate Change 2014: Impacts, Adaptation, and Vulnerability. Part A: Global and Sectoral Aspects. Contribution of Working Group II to the Fifth Assessment Report of the Intergovernmental Panel on Climate Change, pages 1–32. Cambridge University Press, Cambridge, United Kingdom and New York, NY, USA

Kamphuis, J.W., 2000. Shore Protection. In: Introduction to coastal engineering and management. Singapore. World Scientific.

Kench, P. S. and Brander, R. W. , 2006. Response of reef island shorelines to seasonal climate oscillations: South Maalhosmadulu atoll, Maldives. Journal of Geophysical Research: Earth Surface , 111(F1). 190

Kench, P. S., Parnell, K. E., and Brander, R. W., 2009. Monsoonally influenced circulation around coral reef islands and seasonal dynamics of reef island shorelines. Marine Geology, 266(1-4):91–108.

Lesser, G. R., Roelvink, J. A., van Kester, J.A.T.M., Stelling, G. S., 2004. Development and validation of a three-dimensional morphological model. In: Coastal Engineering 51 (8-9), S. 883–915. DOI: 10.1016/j.coastaleng.2004.07.014.

Lewis, J., 1990. The Vulnerability of Small Island States to Sea Level Rise: The Need for Holistic Strategies. Disasters, 14(3), 241–249. doi:10.1111/j.1467-7717.1990.tb01066.x

Lowe, R. J., Falter, J. L., Monismith, S. G., and Atkinson, M. J., 2009. A numerical study of circulation in a coastal reef-lagoon system, J. Geophys. Res., 114, C06022, doi:10.1029/2008JC005081.

Luijendijk, A., Hagenaars, G., Ranasinghe, R., Baart, F., Donchyts, G., & Aarninkhof, S., 2018. The State of the World's Beaches. Scientific Reports, 8(1). doi:10.1038/s41598-018-24630-6

Magnan, A. K., Schipper, E., Burkett, M., Bharwani, S., Burton, I., Eriksen, S., Gemenne, F., Schaar, J. and Ziervogel, G., 2016. Addressing the risk of maladaptation to climate change. WIREs Clim Change, 7: 646-665. doi:10.1002/wcc.409

McLean, R. and Kench, P., 2015. Destruction or persistence of coral atoll islands in the face of 20th and 21st century sea-level rise? Wiley Interdisciplinary Reviews: Climate Change, 6(5):445–463

Naeem, H., 2006. Foahmulaku Beach Erosion & Coastal Protection Report. Ministry of Environment, Energy and Water. Published: 5 June 2006.

Nurse, L. A., McLean, R. F., Agard, J., Briguglio, L. P., Duvat-Magnan, V., Pelesikoti, N., Tompkins, E., and Webb, A., 2014. Small Islands. In Barros, V. R., Field, C. B., Dokken, D. J., Mastrandrea, M. D., Mach, K. J., Bilir, T. E., Chatterjee, M., Ebi, K. L., Estrada, Y. O., Genova, R. C., Girma, B., Kissel, E. S., Levy, A. N., MacCracken, S., Mastrandrea, P. R., and White, L. L., editors , Climate Change 2014: Impacts, Adaptation, and Vulnerability. Part B: Regional Aspects. Contribution of Working Group II to the Fifth Assessment Report of the Intergovernmental Panel of Climate Change, pages 1613–1654. Cambridge University Press, Cambridge, United Kingdom and New York, NY, USA.

Pelling, M., & Uitto, J. I. ,2001. Small island developing states: natural disaster vulnerability and global change. Environmental Hazards, 3(2), 49–62. doi:10.3763/ehaz.2001.0306

Pomeroy, A. W. M., Lowe, R. J., van Dongeren, A. R., Ghisalberti, M., Bodde W., Roelvink, D., 2015. Spectral wave-driven sediment transport across a fringing reef, Coastal Eng. 98, 78–94, doi:10.1016/j.coastaleng.2015.01.005.

Ranasinghe, R., Turner, I.L., 2006.Shoreline response to submerged structures: A review. Coastal Engineering, Volume 53, Issue 1, January 2006, Pages 65-79, https://doi.org/10.1016/j.coastaleng.2005.08.003

Van Rijn, L.C., 1993. Principles of sediment transport in rivers, estuaries and coastal seas. Aqua Publications, the Netherlands

Roeber, V., & Cheung, K. F. ,2012. Boussinesq-typemodel for energetic breaking waves in fringing reef environments. Coastal Engineering,70, 1–20.doi:10.1016/j.coastaleng.2012.06.001.

Roelvink, JA., 2006. Coastal morphodynamic evolution techniques. Coastal Engineering, 53(2-3), 277-287. https://doi.org/doi:10.1016/j.coastaleng.2005.10.015

Soulsby R. L., 1997. Dynamics of Marine Sands. A Manual for Practical Applications, Thomas Telford Publications, Thomas Telford Services Ltd; London.

Storlazzi, C.D., Elias, E., Field, M.E., Presto M.K., 2011. Numerical modeling of the impact of sea-level rise on fringing coral reef hydrodynamics and sediment transport. Coral Reefs 30:83–96DOI 10.1007/s00338-011-0723-9

Storlazzi, C. D., Elias, E. P., and Berkowitz, P., 2015. Many atolls may be uninhabitable within decades due to climate change. Sci Rep, 5:14546.

Storlazzi, C. D., Gingerich, S. B., van Dongeren, A., Cheriton, O. M., Swarzenski, P. W., Quataert, E., Voss, C. I., Field, D. W., Annamalai, H., Piniak, G. A., and McCall, R., 2018. Most atolls will be uninhabitable by the mid-21st century because of sea-level rise exacerbating wave-driven flooding. Science Advances, 4(4)

v. d. Wegen, M., Roelvink, J. A., 2012. Reproduction of estuarine bathymetry by means of a process-based model: Western Scheldt case study, the Netherlands. Geomorphology, Volume 179, Pages 152-167, ISSN 0169-555X, https://doi.org/10.1016/j.geomorph.2012.08.007.

Wessel, P., and J. F. Luis, 2017. The GMT/MATLAB Toolbox, Geochem. Geophys. Geosyst., 18, 811-823.